Linking changes in tectonic style with magmatism in northern Europe during the late Carboniferous to latest Permian

Cite As: Timmerman, MJ, Heeremans, M, Kirstein, LA, Larsen, BT, Spencer-Dunworth, E-A & Sundvoll, B 2009, 'Linking changes in tectonic style with magmatism in northern Europe during the late Carboniferous to latest Permian' *Tectonophysics*, vol 473, no. 3-4, pp. 375-390.

Linking changes in tectonic style with magmatism in northern Europe during the late Carboniferous to latest Permian.

Martin Jan Timmerman [1]

Michel Heeremans[2]

Linda A. Kirstein[3]

Bjørn Tore Larsen[4]

Elizabeth-Anne Spencer-Dunworth[5]

Bjørn Sundvoll[6]

1. Institut für Geowissenschaften, Universität Potsdam, Karl-Liebknecht-Strasse 24, House 27, D-14476 Potsdam, Germany
2. Department of Geosciences, University of Oslo, P.O. Box 1047 Blindern, N-0316 Oslo, Norway
3. Institute of Earth Science, Grant Institute, University of Edinburgh, The King's Buildings, West Mains Road, Edinburgh EH9 3JW, Great Britain
4. Det Norske Oljeselskap ASA, P.O. Box 2070 Vika, 0125 Oslo, Norway
5. Carleton University, Department of Earth Sciences, 2125 Herzberg Building, 1125 Colonel By Drive, Ottawa, Ontario, K1S 5B6, Canada
6. Natural History Museum, University of Oslo, P.O. Box 1172 Blindern, 0318 Oslo

Corresponding author:
Dr. M.J. Timmerman
Institut für Geowissenschaften
Universität Potsdam
Karl-Liebknecht-Strasse 24, House 27
D-14476 Potsdam
Germany

timmer@geo.uni-potsdam.de
Tel.: +49-331-977-5877
Fax: +49-331-977-5821

Abstract

Introduction

Carboniferous-Permian magmatism associated with rifting within the northern foreland of the Variscan orogenic belt is widespread across Europe. On a regional scale magmatism at the end Carboniferous (Stephanian) – Early Permian (~295 Ma) was voluminous with estimates of extruded and intruded magmatic products of approximately 35, 000 km^3 (Ramberg & Larsen, 1978; Kirstein et al., 2006). Smaller regional magmatic events have been documented in the British Isles and Baltic Sea during the Early Carboniferous (~340 Ma) (Timmermann, 2004). To date a range of chronometers have been applied to determine eruption ages from across the region including whole rock Rb/Sr and K/Ar dating (Priem et al., 1968; Neumann et al., 1985; Sundvoll et al. 1990), Ar/Ar dating of mineral separates (Monaghan & Pringle, 2004) and U-Pb dating of perovskite (Corfu and Dahlgren, 2008). The duration of activity has not been previously well-constrained and is currently estimated to span a period of ~100 million years from Early Carboniferous to Early Triassic with several hiatus in activity (Upton et al., 2004).

During the proposed 100 million years of magmatic activity the regional tectonic setting changed across northern Europe. Extensional tectonics, and in particular basin formation and a rifting-wrenching style of deformation occurred across northern Europe from the Carboniferous to Early Permian (McCann et al., 2006, Ziegler et al., 2006). Structural patterns that occur in the northern North Sea are similar to those in the Oslo Rift and Skaggerak-Kattegat areas suggesting similar regional tectonics (Heeremans & Faleide, 2004). During late Permian times thermal relaxation and the development of the Northern and Southern Permian Basins occurred (Glennie, 1998; Van Wees et al., 2000, Frederiksen et al., 2001), as a response to changes in the regional stress pattern.

In this paper we present new $^{40}Ar/^{39}Ar$ step-heating mineral and whole rock ages for volcanic and sub-volcanic rocks from the Oslo Rift, south Sweden (Västergotland and Scania) and north Germany (Rügen) with the aim of improving estimates of the duration of activity in these areas. We document a change in the focus of magmatic activity through time which ultimately centred in the Oslo Rift during the final stages of magmatic activity and propose that changes in regional stress patterns through time play an important role in concentrating magmatic activity in the region.

Regional setting and chronology

Figure 1 shows an overview of the study areas. The study areas are located on the north-eastern part of the Permian Basins.

Oslo Graben, south-east Norway

The Oslo Graben is the onshore part of the Oslo Rift, which extends further south into the offshore Skagerrak Graben (Fig. 1). In the Oslo Graben, several stages of magmatism have been recognized and dated (Sundvoll et al. 1990; Sundvoll & Larsen 1995; Neumann et al. 2004; Larsen et al. 2008). The initial stages comprise the emplacement of fine-grained leucocratic syenite ("mænaite") sills and the extrusion of up to 1500 m of highly and mildly SiO_2 undersaturated to transitional mafic lavas and tuffs in the southern parts of the Oslo Rift (the B1 lavas of the Skien, Brunlanes, Vestfold, and Jeløya areas) (Neumann et al. 2002; Neumann et al. 2004). Corfu and Dahlgren (2008) report three ca. 300 ± 1 Ma U-Pb perovskite and titanite ages for early melilitite and nephelinite flows and tuffs from the basal parts of the Brunlanes sequence in the southernmost parts of the Oslo Graben. Melilite tuff from the base of the Skien succession further north yielded a 299 ± 0.7 Ma U-Pb perovskite age. B1 basalt from the Krokskogen area north of Oslo has a 291 ± 8 Ma Rb-Sr whole rock isochron age (Sundvoll et al. 1990).

In the southern and central parts of the graben, the mafic volcanism was accompanied by the intrusion of small, but widespread mænaite sills that intruded Precambrian gneisses of the basement, lower Palaeozoic sediments, and Westphalian sediments of the Asker Group. Sundvoll et al. (1992) obtained 294 ± 7 Ma to 304 ± 8 Ma Rb-Sr whole rock and mineral isochron ages for the mænaites, and Corfu and Dahlgren (2008) cite a 300 ± 1 Ma U-Pb zircon age. These ages confirm that the earliest stage of rifting and magmatism occurred at the Carboniferous-Permian boundary (299.0 ± 0.8. cf. Gradstein et al. 2004). The earliest magmatic rocks therefore post-date the earliest, Westphalian-age sediments of the Asker Group by ca. 10 Ma (Corfu and Dahlgren 2008).

The subsequent main rift stage resulted in the fissure eruption of thick sequences of predominantly feldspar porphyritic latite/trachyandesite flows (rhomb porphyries) that form large lavas plateaus and constitute the largest volume of volcanics in the Oslo Rift. The rhomb porphyry flows have Rb-Sr mineral isochron ages of 294 ± 6 Ma to 276 ± 6 Ma (Sundvoll and

Larsen 1990; Sundvoll et al. 1990). This volcanism was accompanied by block faulting and intrusion of large amounts of syenitic magmas; Dahlgren et al. (1996) cite 292 ± 0.8 Ma and 299 ± 1.4 Ma U-Pb zircon and baddeleyite ages for two syenite intrusions.

Following the main stage of magmatism, intrusion of dykes and composite batholiths of syenitic to granitic composition took place over a long period. Batholith emplacement was related to the collapse of large shield volcanoes, the local eruption of bimodal, basalt to rhyolite volcanics, and the formation of circular faults and ring dykes outlining collapsed calderas. Ring dykes, central plugs, lavas and granite intrusions have Rb-Sr ages in the range 280 to 241 Ma (Rasmussen et al. 1985; Sundvoll and Larsen 1990; Sunvoll et al. 1990). Larvikite and monzonite intrusions in the southern and south-western Oslo Rift have yielded 277–281 Ma U-Pb zircon and baddeleyite, 277-281 Ma Rb-Sr whole rock and biotite isochron ages (Rasmussen et al. 1985; Sundvoll and Larsen 1990; Sunvoll et al. 1990; Pedersen et al. 1995; Willigers et al. 2004). Neumann et al. (1985) obtained 266 ± 6 Ma and 265 ± 11 Ma Rb-Sr whole rock and mineral isochron ages for small gabbroic intrusions in the NW part of the Vestfold segment (Hadeland). Dolerite and rhomb porphyry dykes intruded Precambrian rocks extend far outside the Oslo Rift (Sundvoll and Larsen 1993, and references therein). Ihlen et al. (1984) obtained 237 ± 4 Ma to 276 ± 5 Ma K-Ar whole rock ages for dolerite dykes near Kongsberg on the western shoulder of the Oslo Rift, preferring a 270 ± 8 Ma mean age for least altered samples.

Youngest magmatism was mainly of granitic to syenitic composition and concentrated in central and northern part of the rift. Here, Sundvoll and Larsen (1990) and Sunvoll et al (1990) report Rb-Sr whole rock isochron ages as young as 241 ± 3 Ma. Torsvik et al. (1998) report ca. 243 ± 5 Ma, Permo-Triassic $^{40}Ar/^{39}Ar$ whole-rock and feldspar ages for two diorite and monzonite dyke that intruded deformed, late Ordovician limestones in the northernmost part of the rift. Magmatism in the Oslo Rift stopped after ca. 240 Ma, having lasted more than 50 Ma (Sundvol et al. 1990).

Combined the data suggest episodic extrusion and intrusion pre and post the voluminous magmatic episode in the Late Carboniferous-Early Permian (~295 ± 5 Ma) with ages ranges from 240 to 280 Ma.

Interpretation of seismic data from the offshore Skagerrak Graben has revealed the presence of half graben geometries below Triassic sedimentary rocks. In addition, the seismic

reflection pattern suggests the presence of thick lava sequences on top of Cambro-Silurian sedimentary rocks comparable with what we observe in the Oslo Graben and other better documented areas such as the North Sea and the Norwegian-Danish Basin (Heeremans and Faleide, 2004).

Västergotland, south Sweden

Dolerite sills in Västergotland in south Sweden intruded Cambro-Silurian sediments that were unconformably deposited in shallow water environments on a peneplain of Precambrian rocks (e.g. Mulder 1971, Nielsen and Schovsbo 2007). The up to 50 m thick, gently NW-dipping Hunneberg-Halleberg, Kinekulle and Billingen sills have been preserved as erosion remnants capping table mountains of early Palaeozoic sediments. No feeder channels have been identified. Priem et al. (1968) obtained 291 ± 15 Ma and 283 ± 8 Ma K-Ar whole rock ages for dolerite of the Billingen sill and the Hunneberg sill, respectively (recalculated using decay constants of Steiger and Jäger 1977).

Scania, south Sweden

A c. 70 km wide swarm of north-west trending mafic dykes in south Sweden (Scania, Fig. 1) is mainly composed of sub-alkaline dolerites (basalt, basaltic andesite) with a few occurrences of camptonite and syenite dykes (Kirstein et al., 2006). The dykes intrude Cambrian to Silurian sediments (Nielsen and Schovsbo 2007). Individual dykes can be up to 100 m wide but the majority vary between 1 and 50 m; their total volume has been estimated at c. 4000 km^3 (Obst 1999; Obst et al. 2004). The available K-Ar ages show a large variation, and a c. 294 Ma K-Ar isochron age is generally thought to be close to the emplacement age (Klingspor 1976). Of similar age may be a few isolated, NNW-trending dolerite and picrite dykes on the south-west coast of Sweden (Samuelsson 1971; Kresten et al. 1982) and those on Bornholm island (Obst 2000). The dykes and sills may be related to volcanic rocks met in drill cores in the Kattegat (offshore western Scania, Mogensen 1994), and to those offshore eastern Denmark, interpreted from seismic data as volcanic edifices (Marek 2000).

Rügen island, north Germany

The oldest rocks penetrated by boreholes on Rügen are Lower Palaeozoic sediments that were deformed under anchizone metamorphic conditions around 450-425 Ma ($^{40}Ar/^{39}Ar$ step-heating ages of whole-rock slates samples, Dallmeyer et al. 1999; Hoth et al. 1997). Undeformed Lower Palaeozoic sediments overlying Mesoproterozoic granites with a 1460 ± 3

Ma Pb-Pb zircon age were met in the G14-1 borehole off-shore north Rügen (Obst et al. 2004). The Lower Palaeozoic rocks of the Rügen basement are overlain by Middle-Upper Devonian and Carboniferous clastic sediments and limestones (Hoth et al. 1997; McCann 1999a, b). Younger, late Carboniferous to early Permian rhyolitic to andesitic volcanic and sub-volcanic rocks were met in deep gas and oil prospecting boreholes in southern Rügen, the mainland to the SW, and the Baltic Sea to the east of Rügen. In contrast, mafic magmatic rocks in the form of dolerite dykes and sills and basalt flows are dominant in the centre of the island. The basalt sequence reaches thicknesses of over 300 m in central Rügen. The thickness of individual dolerite sills varies from 1.5 to 145 m, and is 10 m on average. The sills intrude sediments of Ordovician to Upper Carboniferous age (Korich 1989; Table 1 in Hoth et al. 1993) and rhyolitic volcanic rocks in the southern part of Rügen, locally causing contact metamorphism. The basalts occur interbedded with Upper Carboniferous sediments and, in the south, with rhyolitic volcanic rocks. Locally, the magmatic rocks can reach cumulative thicknesses of up to 1000 m suggesting that they were extruded in the Carboniferous at the earliest.

The dolerites are composed of plagioclase, clinopyroxene, olivine (altered), titano-magnetite and rare biotite, and both aphyric and plagioclase phenocryst-bearing varieties are present. Basalts may be aphyric or contain phenocrysts of orthopyroxene (with Cr-spinel inclusions), olivine, or plagioclase; many contain vesicles filled with secondary calcite and/or chlorite. Both basalts and dolerites have sub-alkaline (tholeiitic) compositions with flat, mid-ocean ridge like, chondrite normalized rare-earth element patterns, and basalts and dolerites are considered to be co-genetic (Kramer 1988; Korich 1989; Korich and Kramer 1994; Marx 1994; Plein 1995, and references therein).

Sample strategy

Here we report 14 new Ar-Ar ages obtained from samples in Norway, Sweden and Germany (Rugen) (Fig. 1). They include both whole rock analyses and mineral separate (feldspar, amphibole) analyses.

Oslo Rift, Norway

Sample Fx6x is from a B1 basalt flow belonging to the upper, low-Ti basalts of the F-Series exposed near Horten in the Vestfold sector. The basalt contains plagioclase phenocrysts and is geochemically relatively evolved (Neumann et al. 2002).

OC-3 is from the syenitic ring dyke of the Øyangen caldera associated with Middle Permian lavas. It is composed of clinopyroxene and kaersutite phenocrysts set in a fine-grained feldspar-rich groundmass.

BGS-1 is from a porphyritic trachyte/syenite plug near Borgersetter within the Øyangen caldera. It contains phenocrysts of large, white feldspar, altered clinopyroxene, euhedral kaersutite, and kaersutite-feldspar intergrowths set in purplish, fine-grained feldspar-rich groundmass.

Kol-1 is a fine-grained basalt. The sample is a lose block taken at the base of a large scree below the cuesta of the Kolsås Basalt Member. The basalt contains a few feldspar phenocrysts of up to 5 mm long set in a fine-grained groundmass of clinopyroxene and plagioclase, and scattered in-filled vesicles.

J-3 is was taken from a camptonite sill exposed in a road-side outcrop on the R4 road, ca. 500m south of Jaren village, north of Gran (Hadeland) (Scott 1980; Scott and Middleton 1983). Apart from a few olivine gabbro intrusions and rhomb porphyry dykes (Neumann et al. 1985; Sundvoll and Larsen 1993), this part of the Oslo Rift is characterized by the occurrence of many sills and dykes of camptonite and mænaite ("bostonite" in Brøgger 1894). The camptonites cut both early Palaeozoic sediments and mænaites. The sampled camptonite sill is choked with large kaersutite and clinopyroxene phenocrysts set in a fine-grained groundmass of amphibole and feldspar. In addition, the sill contains xenoliths of baked, Middle Cambrian alum shales and fragments of an earlier phase of finer grained, amphibole phenocryst-bearing camptonite. Major and trace element chemistry of the sill was reported in Kirstein et al. (2006).

BR-1 was sampled from a few meters wide, east-trending lamprophyric dyke that cuts plagioclase phenocryst-bearing, flow textured basalt or dolerite exposed on the south side of Breisjøen lake in the Alnsjøen area in the Nittedal Caldera (Oslo; Fig. 1). This outcrop corresponds to excursion stop 9 of Naterstad (1977). BR-1 contains phenocrysts of euhedral biotite, eu- to subhedral feldspar, and up to 2.5 cm long, euhedral amphibole set in fine-grained groundmass. In additions, it contains centimetre-sized xenoliths of a syenite dyke that intrudes the basalt at the western end of the exposure.

Samples VO-2 and VO-3 are taken from a dolerite dyke at Vollebek, close to the centre of the city of Oslo along the northern side of road 163. The dyke intruded Cambro-Silurian shales and carbonates as well as a syenitic sill of apparent early Permian age. The dyke is approximately 1m wide and contains kærsutite crystals up to 5 cm in size floating in a fine grained matrix. Xenoliths from crystalline basement are also common. Major and trace elements of these samples are reported by Kirstein et al. (2006).

Västergotland, Sweden

Samples Kin-1 and Bil-1 were taken from the sills exposed on Mt. Kinekulle and Mt. Billingen, respectively, SE of lake Vänern in Västergotland (S Sweden). The rocks are dolerites composed of clinopyroxene phenocrysts set in a sub-ophitic matrix of clinopyroxene, plagioclase and opaque minerals. Sample Mös-1 from Mt. Mösseberg in the same area contains clinopyroxene and plagioclase phenocrysts.

Scania, Sweden

Sample Hb-2 was taken from the north side of 2 to 4 m dolerite dyke that strikes north-west and intruded the Cambrian-age Hardeberga Quartzite in Hardeberga quarry, east of Lund, (Scania, south Sweden). The dolerite contains plagioclase phenocrysts and is cut by calcite veinlets.

Rügen island, Germany

Sample 1085/86 was taken from a dolerite sill met in borehole Rn 103h/62 on Rügen, north Germany (Fig. 1). The borehole penetrates Mesozoic sediments and Permian rocks deposited at the northern margin of the NE German Basin.

Analytical methods

Whole-rock samples (Kol-1, 1085/86, Kin-1, Bil-1) and samples containing groundmass plagioclase (Fx6x, Mos-1, Bil-1), feldspar (Hb-2) or amphibole crystals (BGS-1, OC-3, J-3, BR-1, VO-2, VO-3) were crushed in a steel jaw crusher. The crushed samples were subsequently sieved into several grain size fractions, washed with lukewarm tap water containing a few drop of chlorine-free detergent, repeatedly rinsed, and dried overnight. Magnetic grains were removed using a hand magnet. Mineral concentrates were obtained by

direct handpicking under an overview microscope or by repeated passes through a Frantz magnetic separator at increasing field strengths.

In order to remove any carbonate minerals present, the <30/>60 mesh (250-500 microns) or <60/>90 mesh (170-250 microns) grain-size fractions of the whole-rock sample and the amphibole and feldspar concentrates were leached in *c.* 1M HNO_3 for *c.* 10 minutes at room temperature in an ultra-sonic bath. This was followed by repeated rinsing in deionised water, and leaching in *c.* 7% HF for *c.* 10 minutes (maximum) at room temperature in an ultra-sonic bath. This will remove any surface contaminants and will destroy most alteration products in microcracks (e.g. Wartho et al. 1996). Following rinsing in deionised water and drying in an oven at low temperatures, the leached fractions were sieved again to remove fines produced in the ultrasonic bath, and hand-picked using a binocular microscope (up to 40 times magnification). The transparent feldspars were picked against a white background in order to remove those grains containing dark and opaque inclusions, and against a dark background in order to remove grains showing signs of alteration (mostly secondary sericite, appearing as white patches).

The $^{40}Ar/^{39}Ar$ analyses were performed at the University of Leeds (UK) using a double-vacuum, resistance-heated Ta furnace and a modified AEI MS10 mass spectrometer following the procedures described in Guise & Roberts (2002). Approximately 0.02 to 0.06 gram of material was irradiated in high-purity Al foil at the McMaster reactor in Hamilton (Canada; Pidruczny et al. 1994) and at the Risø reactor in Roskilde (Denmark) for 10 hours. Samples BGS-1, OC-3, VO-2 and VO-3 were irradiated at the McMaster facility, and the interference correction factors were $(^{40}Ar/^{39}Ar)_K = 0.02$, $(^{36}Ar/^{39}Ar)_{Ca} = 0.32$ and $(^{37}Ar/^{39}Ar)_{Ca} = 1515$. The other samples were irradiated at the Risø reactor, and the interference correction factors were $(^{40}Ar/^{39}Ar)_K = 0.048$, $^{36}Ar/^{39}Ar)_{Ca} = 0.038$ and $(^{37}Ar/^{39}Ar)_{Ca} = 1492$. For all irradiations, the flux variation over the length of the canister was monitored by co-irradiated biotite standards Tinto (409.2 Ma, Rex & Guise, 1986) and LP-6 (Engels & Ingamell, 1971) and was of the order of 3%. The Tinto standard has been cross calibrated against HB3gr (Turner et al., 1971), Fy12a (Roddick 1983) and MMHb-1 (Alexander et al., 1978), ages used for each of these standards as given in Roddick (1983).

The $^{40}Ar/^{39}Ar$ data were processed using in-house developed software and plotted using "Isoplot for Excel version 2.49" by Ludwig (2001) which uses the decay constants

recommended by Steiger & Jäger (1977). The uncertainties on the total-gas ages include the uncertainty in the irradiation parameter (J) and are reported at 1σ level; the individual gas fractions (heating steps) are reported with analytical uncertainties (1σ level; Table 3). The plateau and weighted-mean age criteria used in this study are those of Ludwig (2001).

Results

Oslo Rift

Groundmass plagioclase from basalt Fx6x from Vestfold has a 279 ± 1.7 Ma plateau age and a 283 ± 5.6 Ma inverse isotope correlation age for plateau-defining steps 3 to 9 (Fig. 2). Despite yielding a plateau age, the convex upward shape of the age spectrum suggests that loss of argon may have taken place. Argon loss was probably related to hydrothermal alteration and the formation of secondary epidote after magmatic plagioclase, which is widespread in the southern part of the Oslo Rift. Therefore, we tentatively interpret the 279 Ma age as a minimum age for the volcanism in the Vestfold area.

Whole-rock sample Kol-1 from Kolsås yielded a 247 ± 1.7 Ma plateau age and a 246 ± 1.4 Ma total gas age (Table 1, Fig. 2). The 230 ± 23 Ma inverse isotope correlation age is imprecise due to clustering of steps 3 to 9 and the poor correlation. This age is surprisingly young, considering that Sundvoll and Larsen (1990) obtained a 291 ± 6 Ma Rb-Sr whole rock isochron age for the B1 basalt flow of the Krokskogen plateau at Kolsås.

Kaersutites OC-3 and BGS-1 from syenitic intrusions in the Øyangen Caldera both yielded early Permian 273 ± 2.8 Ma and 273 ± 2.4 Ma plateau ages, respectively, and similar inverse isotope correlation and total gas ages (Fig. 3, Table 1). Kaersutite phenocrysts sample J-3 from camptonite sill in Hadeland yielded an early Permian 273 ± 2.6 Ma plateau age that overlaps with the inverse isotope correlation and total gas ages (Fig. 3, Table 1). The Ca/K ratios for these three samples are relatively constant for most of the gas fractions, a slight increase in Ca/K at the high-temperature ends of the spectra of J-3 and BGS-1 (Table 1) may be attributed to breakdown and degassing of plagioclase inclusions in the kaersutites.

Amphibole BR-1 from the lamprophyre from south of Lake Breisjoen in the Nittedal caldera has a 251 ± 2.7 Ma weighted mean age (“forced plateau age”). This Permo-Triassic age overlaps within analytical uncertainty with those of kaersutite phenocrysts from mafic dykes VO-2 and VO-3 from Vollebæk that yielded 246 ± 3 Ma and 249 ± 2.4 Ma plateau ages,

respectively. The plateau ages of VO-2 and VO-3 are indistinguishable from their inverse isotope correlation and total gas ages (Fig. 4, Table 1).

Sweden

Whole rock and groundmass plagioclase from the Billingen dolerite sill in south-central Sweden yielded a plateau and weighted-mean age of, respectively, 300 ± 1.6 Ma and 297.5 ± 3.2 Ma (Fig. 5). These are indistinguishable within analytical uncertainty with their respective inverse isotope correlation ages (Fig. 5). Whole rock sample Kin-1 and groundmass plagioclase Mös-1 have very similar plateau ages of 293 ± 1.3 Ma and 298 ± 2.8 Ma (Table 1). Thus, the dolerite sills in south-central Sweden were emplaced between 293 and 300 Ma. Plagioclase phenocrysts from dolerite dyke Hb-2 in Scania yield a younger 283.5 ± 2.8 plateau age (Fig. 5) and a 285 ± 2.2 Ma total gas age (Table 1).

Germany

Dolerite whole-rock sample 1085/86 from borehole Rn 103h/62 on Rügen island yields a 306 ±11 Ma weighted-mean age and a 309 ± 8 Ma inverse isotope correlation age for the high temperature steps 5 to 10. Apparent ages decrease from 1791 Ma for gas fraction 1 to 307 Ma for fraction 5. The Ca/K ratios remain relatively constant until the increase from 27 to 52 at step 9, which is probably due to outgassing of a Ca-rich, high-temperature phase such as plagioclase.

Discussion

Geographic age distribution

Outside the Oslo Rift and southern Sweden, mafic magmatic activity during the Late Carboniferous (Stephanian (300-286 Ma)) mainly occurred in the form of dolerite dykes and sills in Great Britain and the North Sea. The largest of these, the Whin Sill Complex (WSC, Figs. 1, 6) in northern England comprises a series of dolerite sills and four major ENE trending, en echelon dykes (Thorpe & Macdonald 1985; Johnson & Dunham 2001). The WSC is mainly composed of high-Fe sub-alkaline basalt and its minimum age is c. 294 ± 2 Ma, the $^{40}Ar/^{39}Ar$ weighted-mean age for groundmass plagioclase from the Holy Island Dyke (Timmerman and Upton, in preparation). The east-west trending Midland Valley dyke-sill complex in southern Scotland is composed of quartz dolerites of sub-alkaline to transitional composition (Fig. 1; Macdonald et al. 1981; Kirstein et al., 2006) and the dyke swarm extends c. 200 km eastwards into the North Sea, (Smythe 1994). A felsic segregation vein from a sill

yielded a 307.6 ± 4.8 Ma U-Pb zircon crystallization age (Monaghan and Parrish 2006). In the central North Sea, basalts and tuffs of the up to 160 m thick Inge Volcanics Formation occur interbedded with Rotliegend mud- and sandstones (Glennie 1999). One basalt flow from the Inge Volcanics Formation yielded a c. 299 ± 3 Ma $^{40}Ar/^{39}Ar$ age (Heeremans et al. 2004).

These dyke/sill intrusions reflect a waning of magmatic activity in Britain which had begun more than 50 million years previously with the eruption of the voluminous Clyde Plateau Lavas and petered out of the middle Permian (Monaghan & Pringle, 2004; Upton et al., 2004).

Stephanian to early Permian aged volcanic and sub-volcanic rocks are also known in northern Germany from numerous exploration wells; in north-east Germany these can reach thicknesses of over 2 km (Marx et al. 1995; Benek et al. 1996; Geißler et al. 2008). Rhyolites, which represent the largest volume of the volcanic rocks, have U–Pb zircon crystallization ages in the range 290 ± 3 Ma to 302 ± 3 Ma (Breitkreuz & Kennedy 1999; Breitkreuz et al. 2006). The 306 ±11 Ma Ar/Ar age presented in this paper coincides well with the earlier published ages. Many smaller basins in the internal parts of the Variscan orogen to the south also contain Stephanian to early Permian (sub-) volcanic rocks of felsic to intermediate composition (summarised in Timmerman 2004, 2008). These are dominantly crustal melts resulting from over thickening of the crust in the Variscan fold belt and magmatic underplating (Breitkreuz & Kennedy, 1999).

Emplacement of the dolerite sills in south-central Sweden occurred contemporaneously (295 ± 5 Ma at Billingen, Kinekulle and Mösseberg) and was coeval to the earliest mafic volcanism in the Oslo Rift to the west (Corfu & Dahlgren 2008). Although the mafic melts passed through old and K-rich and, hence, ^{40}Ar-rich Palaeoproterozoic crust and due to their high temperature (ca. 1000°C) may be expected to have partly out-gassed the country rocks, no sign of such old, excess argon is seen in the argon ratios of the low-temperature heating steps. In contrast, sample 1085/86 from borehole 103h/62 on Rügen did incorporate excess argon that was completely released during the low temperature steps. The 286 ± 17 $^{40}Ar/^{36}Ar$ intercept value from the correlation diagram calculated from gas fractions 5 to 10 overlaps with that of air (295.5), indicating the absence of an older argon component.

The age obtained for the emplacement of one of the dykes in the large dyke swarm of Scania, i.e. 283.5 ± 2.8, shows a prolonged magmatic activity into the early Permian.

A second cluster of ages around 275 ± 5 Ma is also evident from the analysed selection of samples. These ages overlap with previously less well constrained events in Norway. The 273 ± 2.8 Ma plateau age for kaersutite OC-3 from the syenite ring dyke of the Øyangen caldera overlaps with the 266 ± 8 to 271 ± 3 Ma Ma Rb-Sr whole rock isochron ages obtained by Sundvoll and Larsen (1990) and Sundvoll et al. (1990) for syenites from the same area. It appears that caldera collapse, ring dyke emplacement and intrusion of late syenite plugs in this part of the Oslo Rift occurred around ca. 273 Ma. The 273 ± 2.6 Ma $^{40}Ar/^{39}Ar$ plateau age for kaersutite J-3 indicates that emplacement of the camptonite sills in Hadeland and may have been related by the collapse of the Øyangen caldera although this is also a minimum age for volcanism in the Vestfold area (Fig. 2).

Finally we can confirm the timing of intrusion of a number of syenites, sills and dykes in southern Norway as being Late Permian. The Permo-Triassic 251 ± 2.7 Ma weighted mean age for amphibole BR-1 from the lamprophyre in the Nittedal caldera overlaps with published Rb-Sr whole rock isochron ages for several syenite varieties from the same general area: 252 ± 3 Ma for a quartz-bearing syenite intrusion (Nittedal nordmarkite; Rasmussen et al. 1985), 255 ± 4 Ma for a syenite intrusion (Grefsen syenite; Sundvoll et al. 1990) and 249 ± 3 Ma for a fine-grained, per-alkaline granite dyke (Storhaug grorudite; Sundvoll and Larsen 1993). Contemporaneous with this activity was the intrusion of the alkalic dykes at Vollebek (VO-2 and VO-3; 246.5 ± 0.46 Ma and 249.18 ± 0.23 Ma resp.) and two dykes at Hadeland (243 ± 5 Ma, Torsvik et al., 1998) suggesting another discrete period of magmatic activity occurred at this time.

Tectonic framework

Regional stress patterns across western and central Europe changed fundamentally in the Late Carboniferous (~295 Ma) (Ziegler, 1990; Ziegler et al., 2004). This change was coincident with the end of orogenesis in the fold belt and a major dextral translation between North Africa and Europe (Wilson et al., 2004). Rifting propagated across basement terranes that varied in thickness and structure from Laurentia in the west to Baltica in the east. Uplift across these terranes was induced in the Late Carboniferous by a complex combination of wrench-related lithospheric deformation, magmatic inflation and basal erosion of the lithosphere (van Wees et al., 2000). Wrench tectonics and faulting was a feature of the Late Carbonigferous when magmatic extrusion, intrusion and underplating were widespread

(Downes, 1993; Wilson et al., 2004). A major change in tectonic style occurred in the Early Permian with the termination of wrench tectonics and thermal contraction of the lithosphere leading to development of the Northern and Southern Permian Basins (van Wees et al., 2000, Frederiksen et al., 2001, Heeremans et al., 2004).

The northern rim of the northern Permian Basin is defined by the Sorgenfrei-Tornquist Zone. This zone separates juvenile sedimentary basins from the stable Fennoscandian craton. Mogensen (1994) has documented right-lateral wrench tectonics during the late Carboniferous – early Permian in the STZ by carefully mapping out the related sedimentary basins in the area. The STZ has probably caused most of the stresses to be transmitted into the northern North Sea (Heeremans et al., 2004). However, some of the stress was also transmitted into the stable craton causing the formation of the Oslo Rift.

Crustal scale fractures provide avenues for magma ascent to the surface. Recurrent disruption of the regional stress field by the prevailing wrench tectonics appears key to facilitate magma generation and eruption/intrusion during the Carboniferous and Permian. The new argon data reported here confirm that magmatic activity across the region can be divided into stages that relate to changes in the regional stress regime.

The cessation of magmatism by the Triassic is consistent with the change in regional stress fields that resulted in a new phase of rifting that accompanied the break up of Pangea (Ziegler et al.,. 2004).

The age obtained for the dyke in Scania, southern Sweden, suggests that these dykes intruded some time after the major magmatic event dominated by wrench tectonics. Bergerat et al. (2007) and Obst (200?) suggested a NE-SW extensional stress regime for this period. Cessation of wrench tectonics and thermal relaxation of the northern Permian Basin could have caused a change in the overall stress regime for this area at that time. At the same time E-W extension prevails further north in the Oslo Graben. This would suggest a decoupling between the stable Fennoscandian craton, affected by E-W extension and the Permian basins were thermal relaxation causes the stress regime to change.

Conclusions

1) Decoupling between Fennoscandian craton where wrench tectonics is succeeded by in general E-W extension during the Permian and the northern Permian Basin where the stress regime changes from right-lateral wrenching to a possible more NE-SW directed extensional stress regime during thermal relaxation of the basin.
2) Ongoing magmatic activity north of the STZ is suggested to be related to ongoing extension in the Fennoscandian craton following the model of Pascal et al. (2004). Magma may have been channelized and trapped into the narrow rift zone.

Acknowledgements

During this research, M.J.T., E.A.S.D., L.A.K. and M.H. were funded by the European Commission TMR Network project "Permo-Carboniferous rifting in Europe" (ERBFMRXCT960093). The authors thank Wolfgang Kramer (GeoForschungsZentrum, Potsdam, Germany) for donating drill core sample 108586 (Rügen).

Table 1 $^{40}Ar/^{39}Ar$ data (MS10 AEI, Leeds University).

Analytical uncertainties are given on 1σ level; uncertainties in total gas age on 2σ level. $^{*40}Ar$ ≡ volume of radiogenic ^{40}Ar; gas volumes corrected to STP. WR = whole rock.

9125.5 WR Leeds run nr. 2489. Sample weight = 0.04614g, J value = 0.00550 ± 0.5 %

Temp °C	$^{39}Ar_K$	$^{37}Ar_{Ca}$	$^{38}Ar_{Cl}$	Ca/K	$^{*40}Ar$	%Atm $^{39}Ar_K$	Age ^{40}Ar	Error	$\%^{39}Ar_K$
	{ Vol. x 10^{-9} cm^3			}				{ Ma	}
554	0.12	0.82	0.011	13.9	28.16	84.1	259.8	32.3	2.3
660	0.44	3.98	0.009	17.9	34.44	15.9	312.9	7.7	8.5
720	0.70	6.81	0.011	19.5	33.49	55.7	305.0	3.4	13.4
786	1.12	10.40	0.015	18.5	32.14	10.8	293.7	3.3	21.5
849	0.87	7.17	0.009	16.4	32.21	9.8	294.2	3.5	16.8
912	0.64	6.51	0.009	20.1	32.79	12.1	299.2	2.9	12.4
980	0.34	3.36	0.005	19.7	33.11	21.8	301.8	12.9	6.6
1050	0.42	2.58	0.007	12.3	31.62	35.4	289.3	12.9	8.1
1145	0.33	5.92	0.007	35.9	32.42	18.9	296.0	12.1	6.3
1289	0.21	11.24	0.008	107.0	33.67	35.8	306.5	10.1	4.0

Total gas age = 298 ± 6 Ma (Weight %K = 0.29, $^{*40}Ar$ = 36.7 x 10^{-7} cm^3g^{-1})

9115.0 WR Leeds run nr. 2484. Sample weight = 0.0550g, J value = 0.00550 ± 0.5 %

Temp °C	$^{39}Ar_K$	$^{37}Ar_{Ca}$	$^{38}Ar_{Cl}$	Ca/K	$^{*40}Ar$	%Atm $^{39}Ar_K$	Age ^{40}Ar	Error	$\%^{39}Ar_K$
	{ Vol. x 10^{-9} cm^3			}				{ Ma	}
560	0.29	1.62	0.020	11.1	35.35	73.6	320.5	14.1	3.0
680	1.44	8.83	0.023	12.2	34.12	35.8	310.3	1.8	15.0
740	1.72	10.81	0.022	12.5	33.39	9.6	304.1	1.0	18.0
820	2.30	10.42	0.032	9.0	32.76	6.8	298.9	1.2	24.1
877	1.27	5.74	0.018	9.0	32.28	12.8	294.9	1.4	13.2
967	0.96	4.56	0.016	9.5	32.29	19.5	293.0	4.6	10.0
1018	0.50	1.88	0.014	7.4	31.15	23.8	285.3	6.5	5.3
1093	0.54	3.52	0.013	13.0	31.28	16.7	286.4	6.8	5.6
1181	0.27	9.40	0.009	70.0	31.23	29.3	286.0	5.9	2.8
1317	0.28	11.18	0.021	79.9	31.22	44.0	285.9	14.0	2.9

Total gas age = 299 ± 4 Ma (Weight %K = 0.45, $^{*40}Ar$ = 57.0 x 10^{-7} cm^3g^{-1})

Table 1. $^{40}Ar/^{39}Ar$ data, MS10, Leeds University. Analytical uncertainties are reported at 1-σ. $^{*40}Ar$ ≡ volume of radiogenic ^{40}Ar, gas volumes corrected to STP. The uncertainties on the total-gas ages include the uncertainty in the irradiation J parameter and are reported at 2σ level. The individual gas fractions are reported with analytical uncertainty at 1σ level, including the uncertainty on the J-value. Abbreviation: t.f. = total fusion.

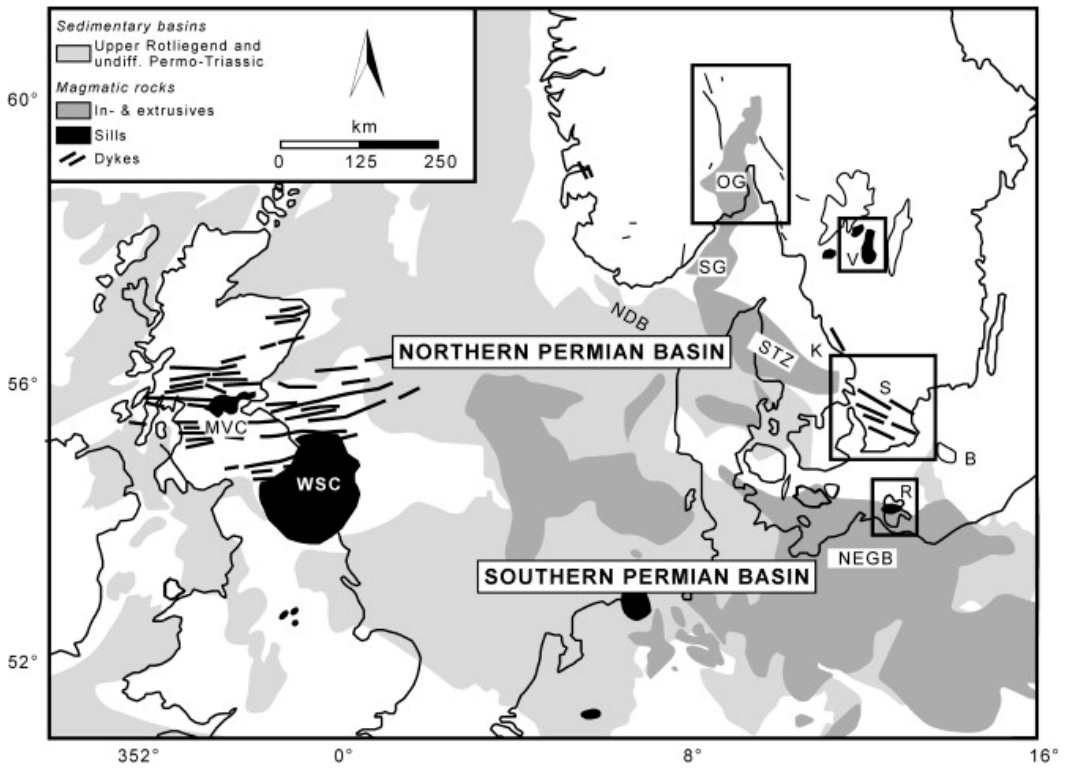

Fig. 1. Overview map of northwestern Europe showing the major late Carboniferous–early Permian magmatic provinces (after Timmerman et al.,2004). Abbreviations: B = Bornholm island; K = Kattegat; MVC = Midland Valley Complex; NDB = Norwegian–Danish Basin; NEGB = NE German Basin; OG = Oslo Graben; R = Rügen island; S = Scania; SG = Skagerrak Graben; STZ = Sorgenfrei–Tornquist Zone; V = Västergotland; WSC = Whin Sill Complex.

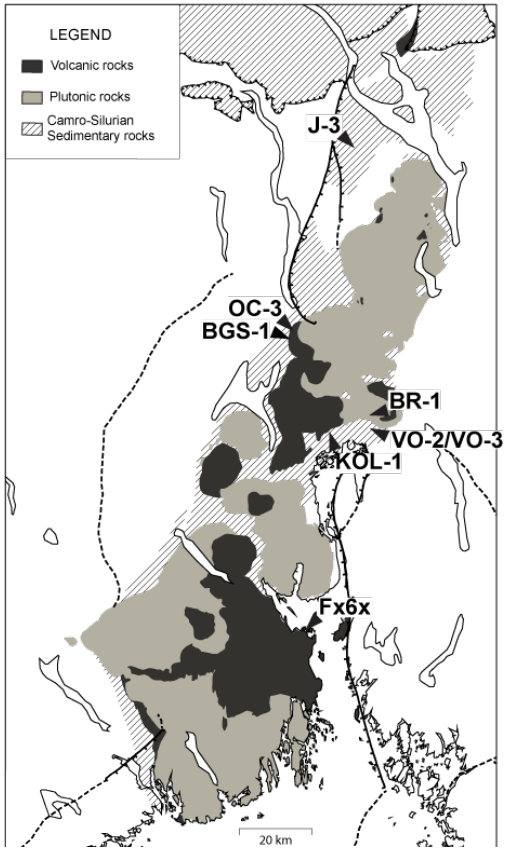

Fig. 2. Simplified geological map of the Oslo Graben (after Ramberg and Larsen, 1978) showing locations of samples J-3, OC-3, BGS-1, BR-1, VO-2, VO-3 and Fx6x. Abbreviations: Ha = Hadeland; Kr = Krokskogen; KB = Kongsberg Block; N = Nittedal caldera; O = Øyangen caldera; V = Vestfold.

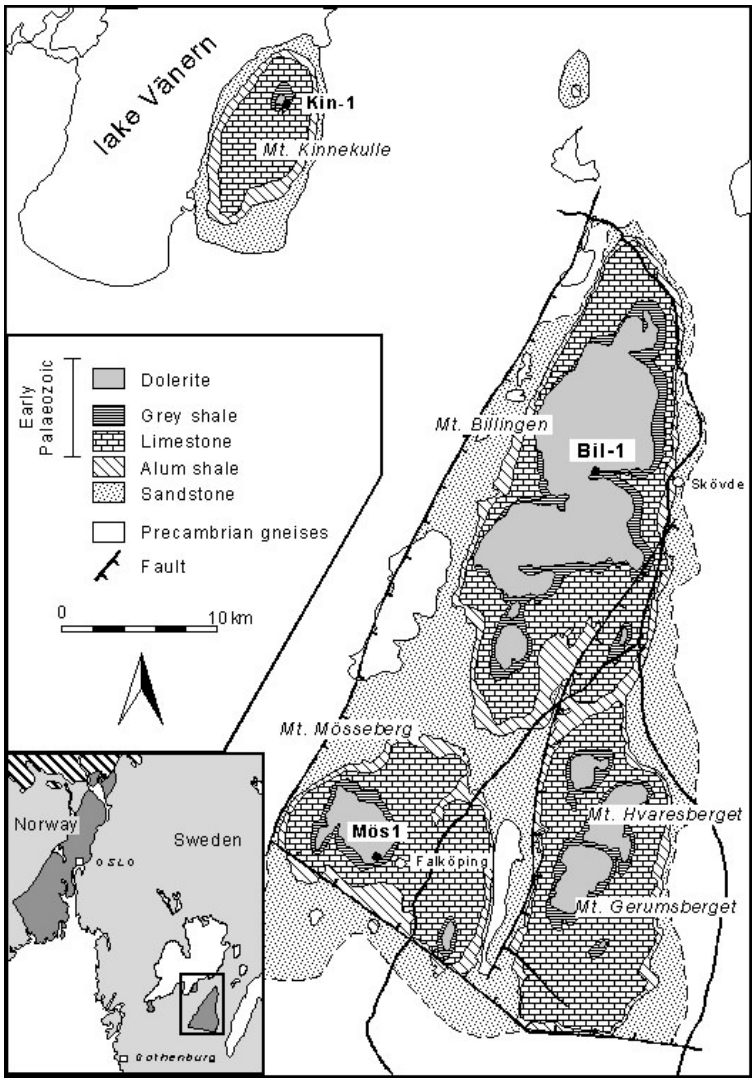

Fig. 3. Geological map of Västergotland, south Sweden, showing Permo-Carboniferous dolerite sills intruding Early Palaeozoic sediments and locations of dolerite samples Bil-1, Kin-1 and Mös-1 (after Munthe et al., 1928).

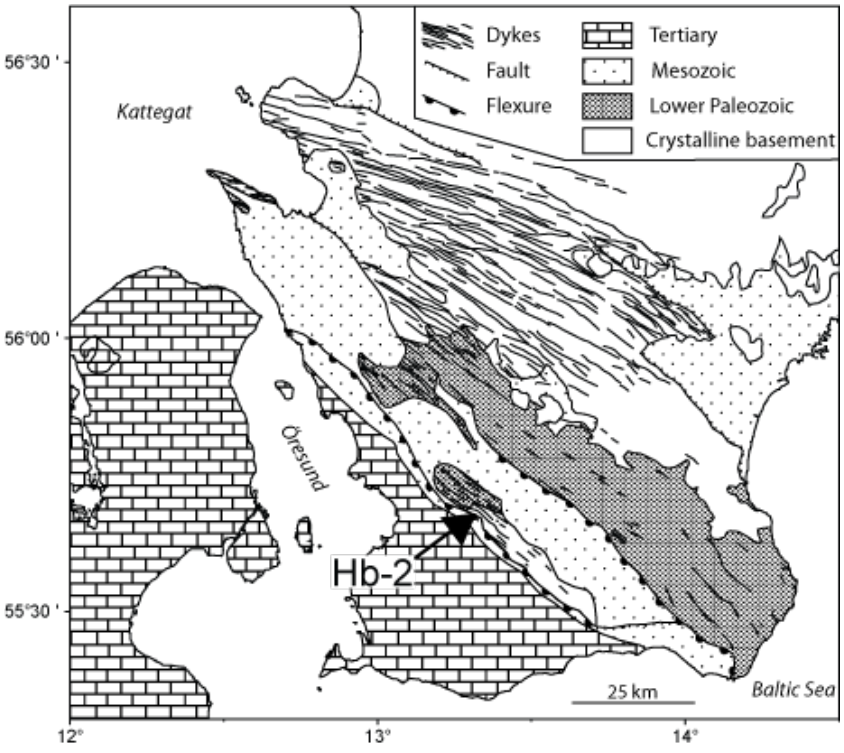

Fig. 4. Geological map of Scania (south Sweden) showing the Permo-Carboniferous dolerite dyke swarm and location of dolerite sample Hb-2 (after Obst et al., 2004).

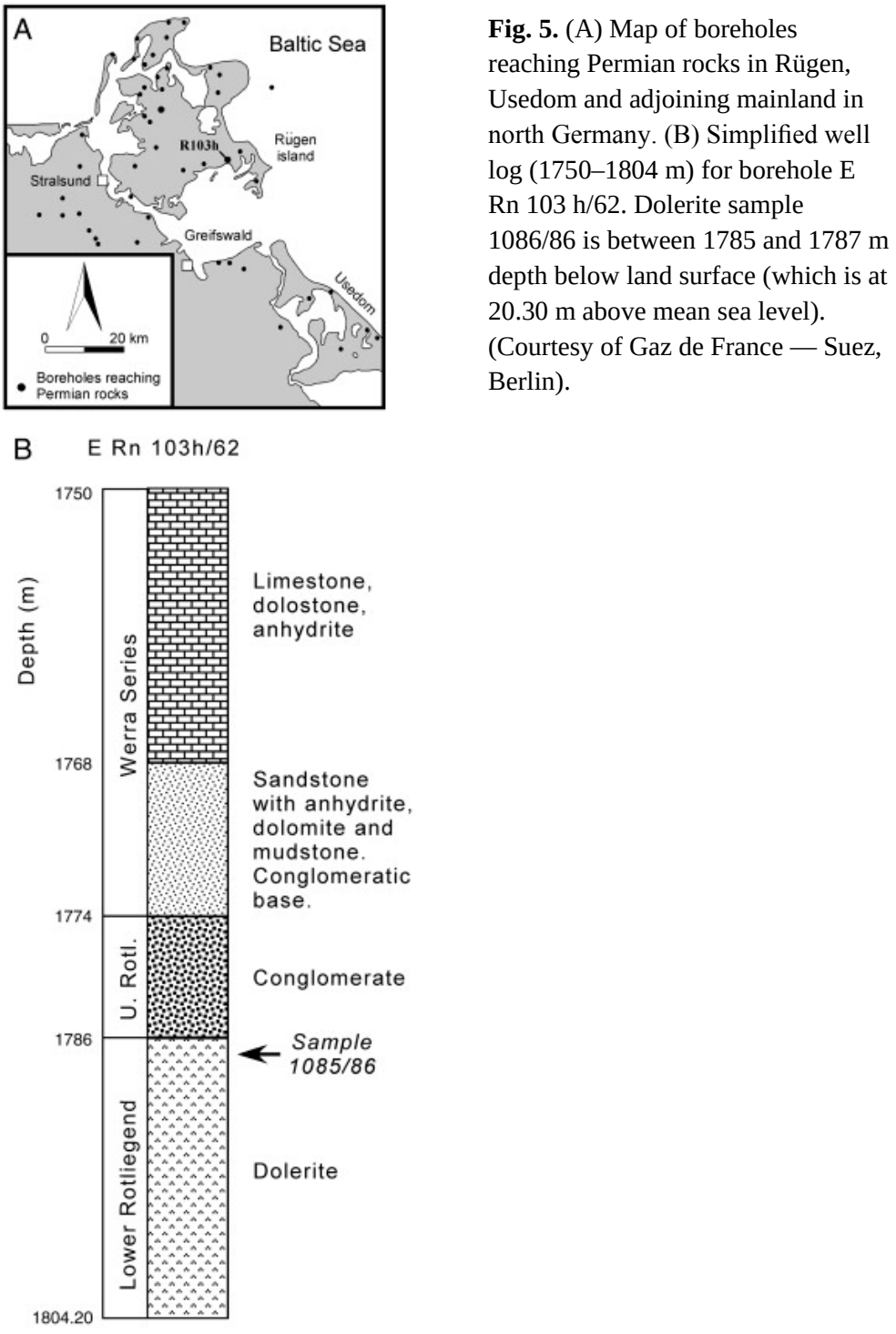

Fig. 5. (A) Map of boreholes reaching Permian rocks in Rügen, Usedom and adjoining mainland in north Germany. (B) Simplified well log (1750–1804 m) for borehole E Rn 103 h/62. Dolerite sample 1086/86 is between 1785 and 1787 m depth below land surface (which is at 20.30 m above mean sea level). (Courtesy of Gaz de France — Suez, Berlin).

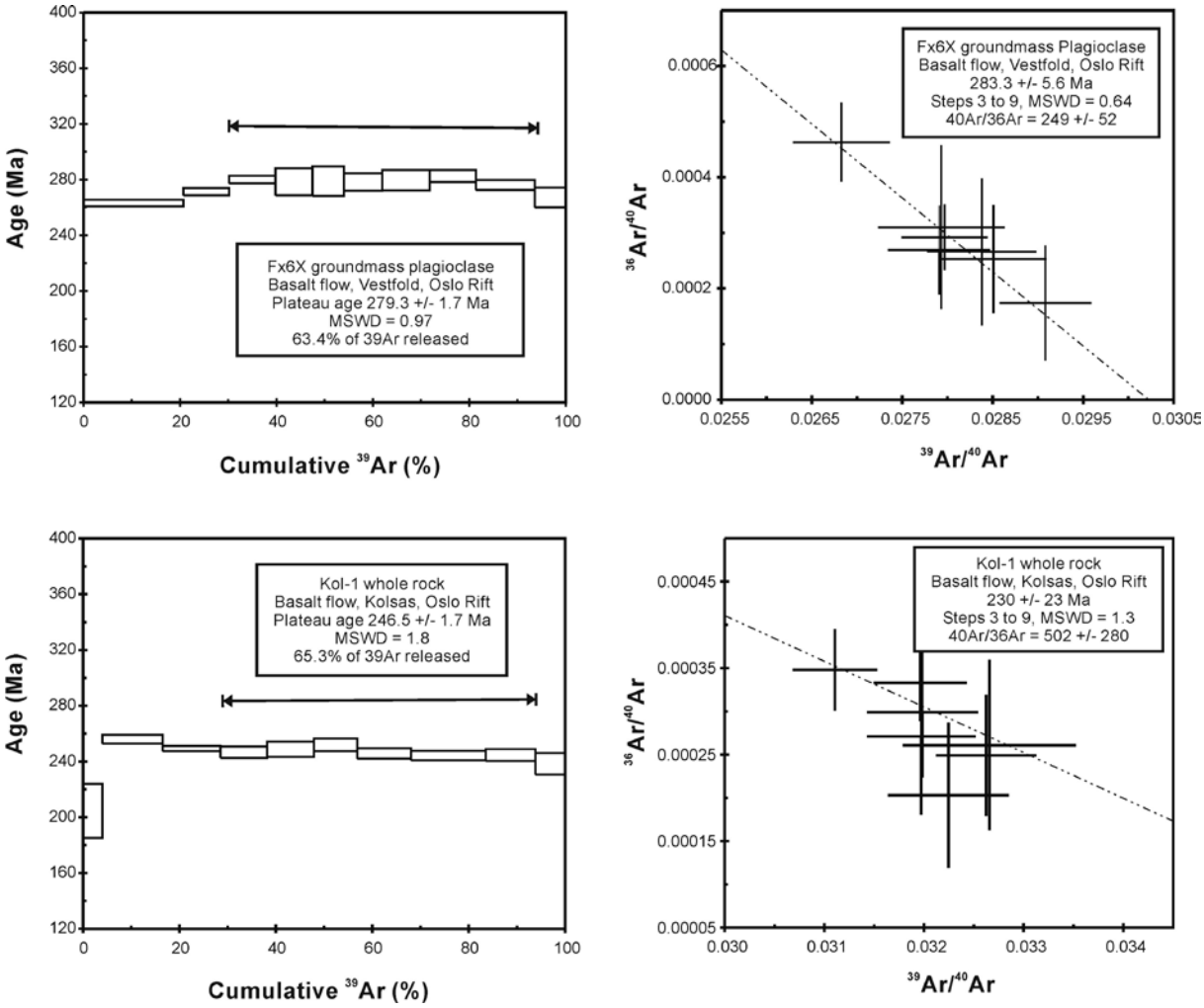

Fig. 6. Argon age spectrum (A) and inverse isotope correlation diagram (B) for the plagioclase fraction from basalt Fx6x, Vestfold area (Oslo Graben). The arrows mark the gas fractions that were used in the plateau and isotope correlation calculations.

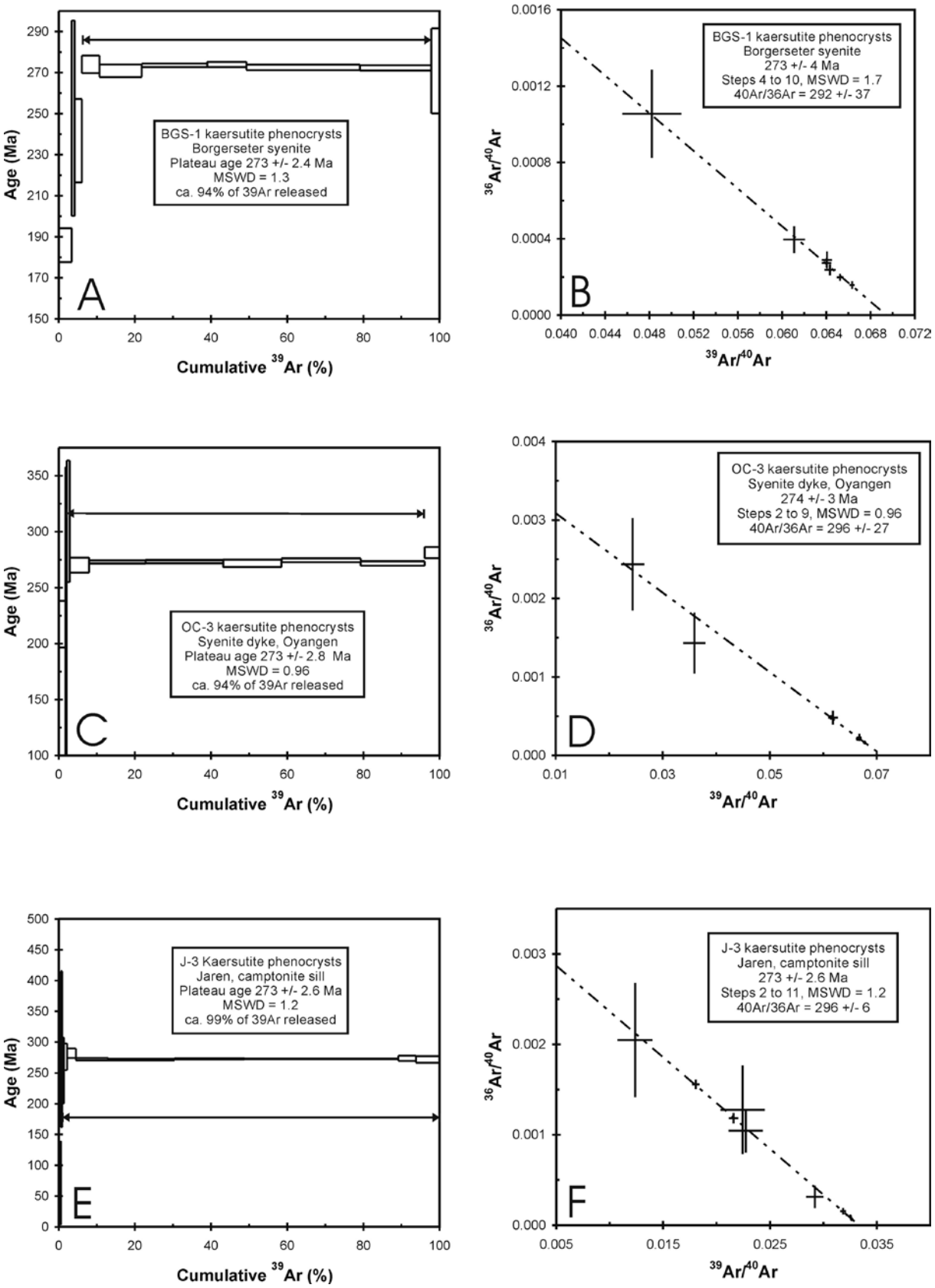

Fig. 7. Argon age spectra and inverse isotope correlation diagrams for kaersutites from the Oslo Graben: (A) and (B) Borgersætra (BGS-1); (C) and (D) Øyangen (OC-3); (E) and (F) Jaren (J-3). The arrows mark the gas fractions that were used in the plateau and isotope correlation calculations.

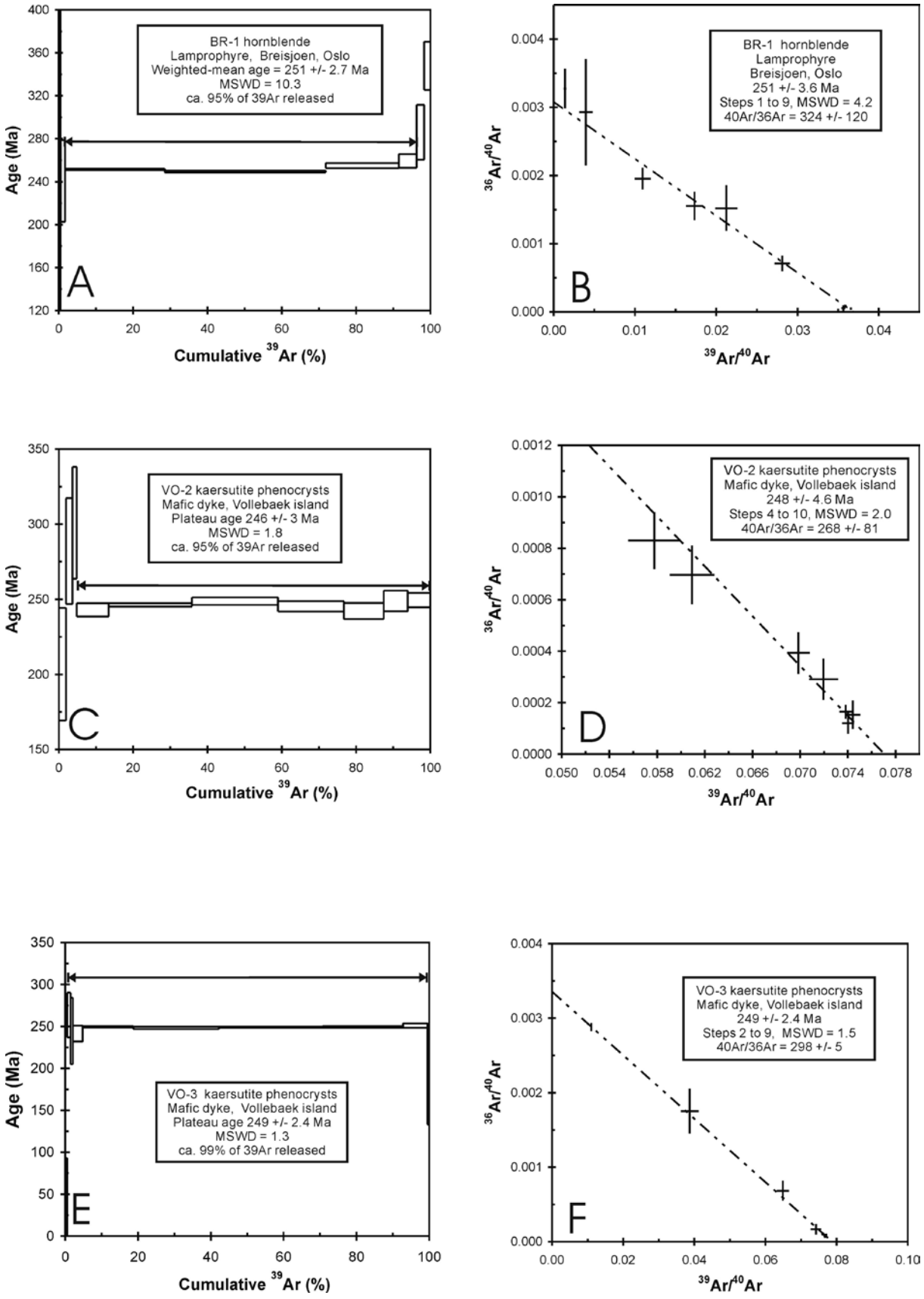

Fig. 8. Argon age spectra and inverse isotope correlation diagrams for amphiboles from the Oslo Graben: (A) and (B) Breisjoen (BR-1); (C) to (F) Vollebæk (VO-2, VO-3) (Oslo). The arrows mark the gas fractions that were used in the plateau, weighted-mean and isotope correlation calculations.

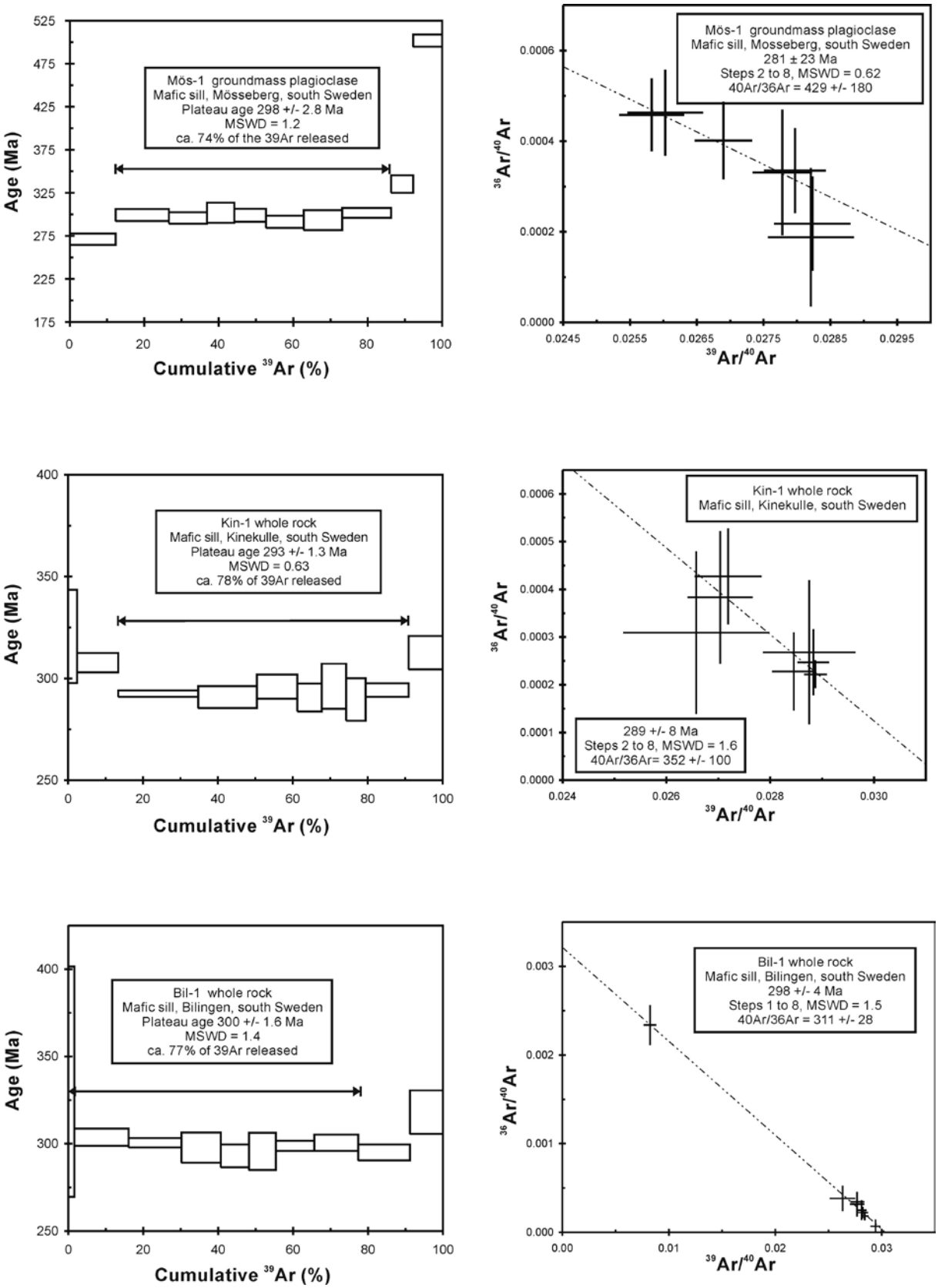

Fig. 9. Argon age spectra and inverse isotope correlation diagrams for a plagioclase fraction and whole-rock samples from Västergotland: (A) and (B) Mösseberg (Mös-1); (C) and (D) Kinekulle (Kin-1); (E) and (F) Billingen (Bil-1). The arrows mark the gas fractions that were used in the plateau and isotope correlation calculations.

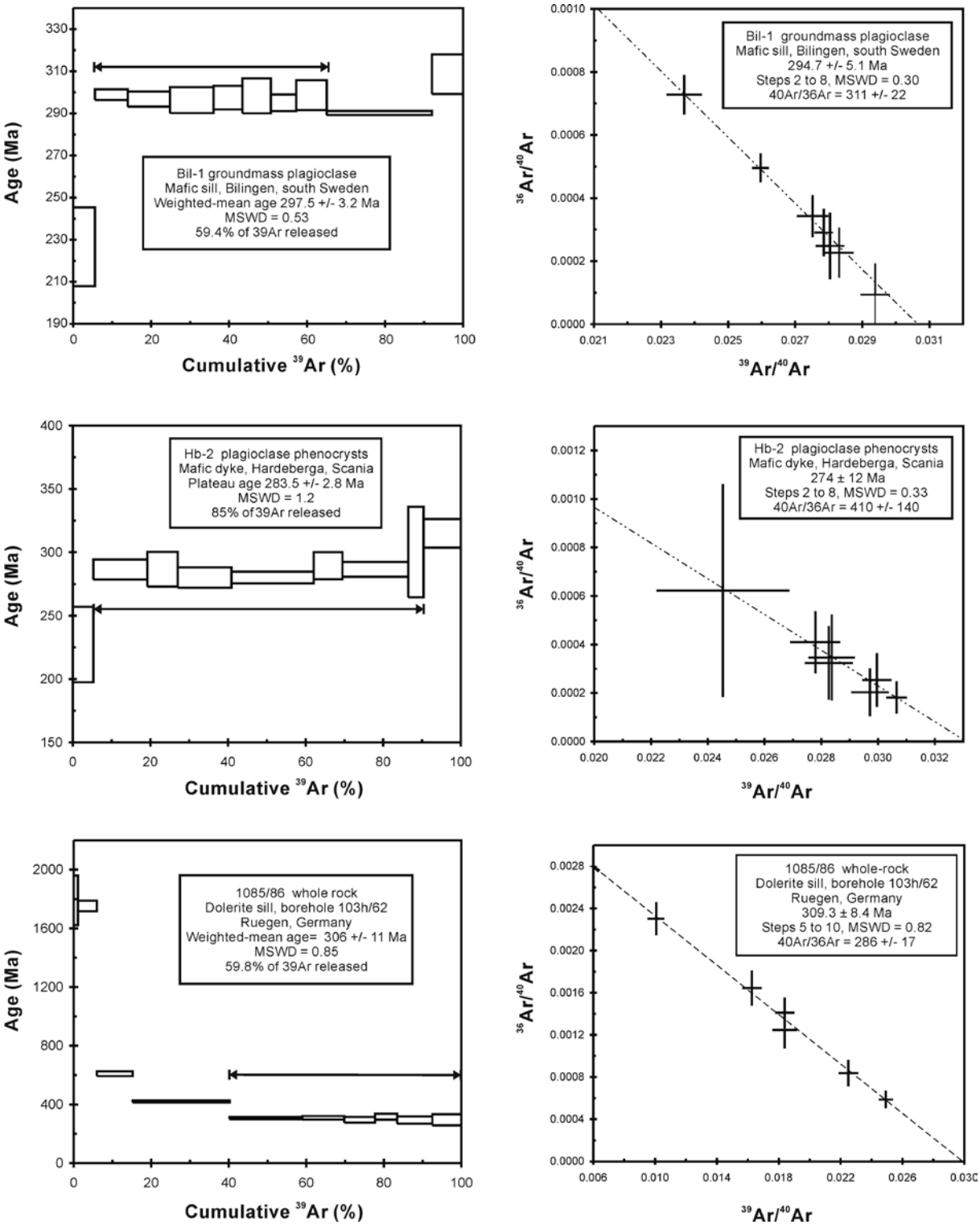

Fig. 10. Argon age spectra and inverse isotope correlation diagrams for plagioclase fraction and whole-rock sample from: (A) and (B) Billingen (Bil-1) (Västergotland); (C) and (D) Hardeberga (Hb-2) (Scania); (E) and (F) borehole E Rn 103 h/62 on Rügen (1085/86) (Germany). The arrows mark the gas fractions that were used in the plateau, weighted-mean and isotope correlation calculations.

References

Alexander Jr., E.C., Mickelson, G.M. and Lanphere, M.A. 1978. MMHb-1: A new ^{40}Ar-^{39}Ar dating standard. *U.S.G.S. Open File Report,* **78-701**, 6-8.

Breitkreuz, C., Kennedy, A., Geissler, M., Ehling, B.-C., Kopp, J., Muszynski, A., Protas, A. and Stouge, S. 2007. Far Eastern Avalonia: its chronostratigraphic structure revealed by SHRIMP zircon ages from Upper Carboniferous to Lower Permian volcanic rocks (drill cores from Germany, Poland and Denmark). In: Linnemann, U., Nance, R.D., Kraft, P. and Zulauf, G. (eds), *The evolution of the Rheic Ocean: from Avalonian-Cadomian active margin to Alleghenian-Variscan collision*. Geological Society of America, Special Paper, **423**, 173-190.

Brøgger, W.C. 1894. The basic eruptive rocks of Gran. *Quarterly Journal of the geological Society, London,* **50**, 15-38.

Corfu, F. and Dahlgren, S. 2008. Perovskite U–Pb ages and the Pb isotopic composition of alkaline volcanism initiating the Permo-Carboniferous Oslo Rift. *Earth and Planetary Science Letters*, **265**, 256–269.

Dahlgren, S. and Corfu, F. 2001. Northward sediment transport from the late Carboniferous Variscan Mountains: zircon evidence from the Oslo Rift, Norway. *Journal of the Geological Society, London,* **158**, 29-36.

Dallmeyer, R.D., Giese,U., Glasmacher, U. and Pickel, W. 1999. First $^{40}Ar/^{39}Ar$ age constraints for the Caledonian evolution of the Trans–European Suture Zone in NE Germany. *Journal of the Geological Society, London,* **156**, 279-290.

Engels, J.C. and Ingamells, C.O. 1971. Information Sheets 1 and 2, LP-6 Biotite 40-60 mesh. *U.S.G.S. Menlo Park*, California U.S.A.

Geißler, M., Breitkreuz, C. and Kiersnowski, H. 2008. Late Paleozoic volcanism in the central part of the Southern Permian Basin (NE Germany, W Poland): facies distribution and volcano-topographic hiati. *International Journal of Earth Sciences,*

Gradstein, F.M., Ogg, J.G., Smith, A.G., Bleeker, W. and Lourens, L.J. 2004. A new Geologic Time Scale, with special reference to Precambrian and Neogene. *Episodes,* **27**, 33-100.

Grimmer, S.C. 1991. Geochemistry and petrography of alkali volcanics from the Oslo Palaeorift, Norway. Unpublished Ph.D. Thesis, University of Keele, Great Britain.

Guise, P.G. and Roberts, D. 2002. Devonian ages from $^{40}Ar/^{39}Ar$ dating of plagioclase in dolerite dykes, eastern Varanger Peninsula, North Norway. *Norges Geologiske Undersokelse, Bulletin,* **440**, 27-37.

Hoth, K., Huebscher, H.-D., Korich, D., Gabriel, W. and Enderlein, F. 1993. Die Lithostratigraphie der permokarbonischen Effusiva im Zentralabschnitt der Mitteleuropäischen Senke. Der permokarbonische Vulkanismus im Zentralabschnitt der Mitteleuropäische Senke, Teil 1. *Geologisches Jahrbuch,* **A131**, 179-196.

Hoth, P., 1997. Fazies und Diagenese von Präperm-Sedimenten der Geotraverse Harz-Rügen. *Schriftenreihe für Geowissenschaften*, **4**, 1-139.

Ihlen, P.M., Ineson, P.R., Mitchell, J.G. and Vokes, F.M. 1984. K-Ar dating of dolerite dykes in the Kongsberg-Fiskum district, Norway, and their relationships with the silver and base-metal veins. *Norsk Geologisk Tidsskrift*, **64**, 87-96.

Kirstein, L.A., Davies, G.R. and Heeremans, M. 2006. The petrogenesis of Carboniferous-Permian dyke and sill intrusions across northern Europe. *Contributions to Mineralogy and Petrology*, **152**, 721-742.

Korich, D., 1989. Zum Stoffbestand jungpaläozoischer basischer Magmatite aus dem DDR-Anteil der Mitteleuropäischen senke. *Zeitschrift für angewandte Geologie*, **35**, 113-138.

Kramer, W. 1988. Magmengenetische Aspekte der Lithosphärenentwicklung. Geochemisch-petrologische Untersuchungen basaltoider variszischer Gesteinsformationen sowie mafischer und ultramafischer Xenolithe im nordöstlichen Zentraleuropa. *Schriftenreihe für geologische Wissenschaften*, **26**, 1-136.

Kresten, P., Samuelsson, L. and Rex, D.C. 1982. Ultramafic dykes on the northern Skagerrak coast of Sweden. *Geologiska Föreningens i Stockholm Förhandlingar*, **103**, 285-289.

Larsen, B.T., 1978. Krokskogen Lava Area. In: Dons, J.A. and Larsen, B.T. (eds), The Oslo paleorift. A review and guide to excursion. *Norges Geologiske Undersokelse*, **337**, 143-162.

Larsen, B.T., Olaussen, S., Sundvoll, B. and Heeremans, M., 2008. The Permo-Carboniferous Oslo Rift through six stages and 65 million years. *Episodes*, **31**, 1-7.

Ludwig, K.R. 2001. Users' manual for Isoplot/Ex rev. 2.49. A Geochronological Toolkit for Microsoft Excel. *Berkeley Geochronology Center, Special Publication*, **1a**, 1-58.

McCann, T., 1999a. Middle to Late Devonian basin evolution in the Rügen area, NE Germany. *Geologie en Mijnbouw*, **78**, 57–71.

McCann, T., 1999b. The tectonosedimentary evolution of the northern margin of the Carboniferous foreland basin of NE Germany. *Tectonophysics*, **313**, 119-144.

Marx, J. 1994. Die permokarbonen Magmatite Nordwestdeutschlands im Vergleich zu den magmatischen Serien angrenzender Gebiete. Unpublished Dissertation, University of Hannover, 197 pp.

Monaghan A. and Pringle M. 2004. $^{40}Ar/^{39}Ar$ Geochronology of Carboniferous-Permian Volcanism in the Midland Valley, Scotland. 2004. In Wilson M., Neumann E-R., Davies G.R. et al. (eds) *Permo-Carboniferous Magmatism and Rifting in Europe*. Geological Society, London, Special Publications, **223**, 219-242.

Monaghan, A.A. and Parrish, R.R. 2006. Geochronology of Carboniferous-Permian magmatism in the Midland valley of Scotland: implications for regional tectonomagmatic evolution and the numerical time scale. *Journal of the geological Society, London*, **163**, 15-28.

Mulder, F.G. 1971. Paleomagnetic research in some parts of central and southern Sweden. *Sveriges Geologiska Undersökelse*, **C653**, 1-56.

Naterstad, J., 1978. Nittedal Cauldron (Alnsjøen Area). In: Dons, J.A. and Larsen, B.T. (eds), The Oslo paleorift. A review and guide to excursion. *Norges Geologiske Undersokelse*, **337**, 99-103. (+ 1 map)

Neumann, E.-R., Larsen, B.T. and Sundvoll, B. 1985. Compositional variations among gabbroic intrusions in the Oslo rift. *Lithos*, **18**, 35-59.

Neumann, E.-R., Dunworth, E.A., Sundvoll, B.A. and Tollefsrud, J.I. 2002. B1 basaltic lavas in Vestfold–Jeløya area, central Oslo rift: derivation from initial melts formed by progressive partial melting of an enriched mantle source. *Lithos*, **61**, 21– 53.

Neumann, E.-R., Wilson, M., Heeremans, M., Spencer, E.A., Obst, K., Timmerman, M.J. and Kirstein, L. 2004. Carboniferous-Permian rifting and magmatism in southern Scandinavia, the North Sea and northern Germany: a review. In: Wilson, M., Neumann, E.-R., Davies, G.R., Timmerman, M.J., Heeremans, M. and Larsen, B.T. (eds.), *Permo-Carboniferous Rifting and Magmatism in Europe*. Geological Society, London, Special Publications, **223**, 11-40.

Nielsen, A.T. and Schovsbo, N.H. 2007. Cambrian to basal Ordovician lithostratigraphy in southern Scandinavia. *Bulletin of the Geological Society of Denmark*, **53**, 47–92.

Obst, K. 1999. Die permosilesischen Eruptivgänge innerhalb der Fennoskandischen Randzone (Schonen und Bornholm). Untersuchungen zum Stoffbestand, zur Struktur und zur Genese. *Greifswalder Geowissenschaftliche Beiträge*, **7/1999**, 1-121.

Obst, K., 2000. Permo-Carboniferous dyke magmatism on the Danish island Bornholm. *Neues Jahrbuch für Geologie und Paläontologie, Abhandlungen*, **218**, 243-266.

Obst, K., Solyom, Z. and Johansson, L. 2004. Permo-Carboniferous extension-related magmatism at the SW margin of the Fennoscandian Shield. *In*: Wilson, M., Neumann, E.-R., Davies, G.R., Timmerman, M.J., Heeremans, M. & Larsen, B.T. (eds) *Permo-Carboniferous Magmatism and Rifting in Europe*. Geological Society, London, Special Publications, **223**, 259-288.

Obst, K., Hammer, J., Katzung, G. and Korich, D. 2004. The Mesoproterozoic basement in the southern Baltic Sea: insights from the G 14–1 off-shore borehole. *International Journal of Earth Science*, **93**, 1–12.

Olausen, S. 1981. Marine incursions in Upper Paleozoic sedimentary rocks of the Oslo Region. Southern Norway. *Geological Magazine*, **118**, 281-288.

Pidruczny, A.E., Butler, M.P., Ernst, P.C., Collins, M.F. and Avelar, J.M. 1994. The McMaster University Nuclear Reactor (MNR) research facilities. *Journal of Radioanalytical and Nuclear Chemistry, Articles,* **180**, 313-318.

Plein, E. (ed.) 1995. Norddeutsches Rotliegend-Becken. Rotliegend Monographie, Teil II. *Courier Forschungsinstitut Senckenberg*, **183**, 1-193.

Priem, H.N.A., Mulder, F.G., Boelrijk, N.A., Hebeda, E.H., Verschure, R.H. and Verdurmen, E.A. 1968. Geochronological and palaeomagnetic reconnaissance survey in parts of central and southern Europe. *Physics of the Earth and Planetary Interiors*, **1**, 373-590.

Rasmussen, E., Neumann, E.-R., Andersen, T., Sundvoll, B., Fjerdingstad, V. and Stabel, A. 1988. Petrogenetic processes associated with intermediate and silicic magmatism in the Oslo rift, southeast Norway. *Mineralogical Magazine*, **52**, 293-307.

Rex, D.C. and Guise, P.G. 1986. Age of the Tinto felsite, Lanarkshire: a possible ^{39}Ar-^{40}Ar monitor. *Bulletin of Liaison and Information*. I.G.C.P. Project 196, No 6, 1986.

Roddick, J. C. 1983. High precision intercalibration of ^{40}Ar-^{39}Ar standards. *Geochimica et Cosmochimica Acta*, **47**, 887-898.

Samuelsson, L. 1971. The relationship between Permian dikes of dolerite and rhomb porphyry along the Swedish Skagerrak coast. *Sveriges Geologiska Undersökning*, **C663**, 1-51.

Scott, P.W. 1980. Zoned pyroxenes and amphiboles from camptonites near Gran, Oslo Region, Norway. *Mineralogical Magazine*, **43**, 913-917.

Scott, P.W. and Middleton, R. 1983. Camptonite and Mænaite sills near Gran, Hadeland, Oslo Region. *Norges Geologiske Undersøkelse*, **289**, 1-26.

Steiger, R.H. and Jäger, E. 1977. Subcommission on geochronology: Convention on the use of decay constants in geo- and cosmochronology. *Earth and Planetary Science Letters*, **36**, 359-362.

Timmerman, M.J. 2004. Timing, geodynamic setting and character of Permo-Carboniferous magmatism in the foreland of the Variscan Orogen, NW Europe. In: Wilson, M., Neumann, E.-R., Davies, G.R., Timmerman, M.J., Heeremans, M. and Larsen, B.T. (eds.), *Permo-Carboniferous Rifting and Magmatism in Europe*. Geological Society, London, Special Publications, **223**, 41-74.

Timmerman, M.J., 2008. Palaeozoic magmatism. In: T. McCann (ed.), *The Geology of Central Europe*. Geological Society of London. (*in press*)

Turner, G., Huneke, J.C., Podosek, F.A. and Wasserburg, G.J. 1971. ^{40}Ar-^{39}Ar ages and cosmic ray exposure ages of Apollo 14 samples. *Earth and Planetary Science Letters*, **12**, 19-35.

Upton, B.G.J., Stephenson, D., Smedley, P.M., Wallis, S.M. and Fitton, J.G. 2004. Carboniferous and Permian magmatism in Scotland. In Wilson M., Neumann E-R., Davies G.R. et al. (eds) *Permo-Carboniferous Magmatism and Rifting in Europe*. Geological Society, London, Special Publications, **223**, 219-242.

Wartho, J.-A., Rex, D.C. and Guise, P.G. 1996. Excess argon in amphiboles linked to greenschist facies alteration in the Kamila Amphibolite Belt, Kohistan island arc system, northern Pakistan: insights from ^{40}Ar/^{39}Ar step-heating and acid leaching experiments. *Geological Magazine*, **133**, 595-609.

Willigers, B.J.A., Mezger, K. and Baker, J.A. 2004. Development of high precision Rb–Sr phlogopite and biotite geochronology; an alternative to ^{40}Ar/^{39}Ar tri-octahedral mica dating. *Chemical Geology*. **213**, 339– 358.

Zeck, H.P., Andriessen, P.A.M., Hansen, K., Jensen, P.K. and Rasmussen, B.L. 1988. Paleozoic paleo-cover of the southern part of the Fennoscandian Shield - fission track constraints. *Tectonophysics*, **149**, 61-66.